Fachhochschule Aachen

Campus Jülich

Fachbereich 10: Energietechnik

Physical Engineering

Dielectric Properties measurement setup and ferroelectric properties of multiferroic Metal-Organic-Frameworks(MOFs) with perovskite architecture

Angefertigt am

Jülich Centre for Neutron Science, JCNS-2,

Und Peter Grünberg Institut,PGI-4:

Streumethoden

Forschungszentrum Jülich GmbH

Bachelorarbeit von Jingdong Guo

Jülich, August, 2016

Diese Arbeit ist von mir selbständig angefertigt und verfasst. Es sind keine anderen als die angegebenen Quellen und Hilfsmittel benutzt worden.

Ort, Datum	eigenhändige Unterschrift

Diese Arbeit wurde betreut von:

1. Prüfer: Prof. Dr. Arnold Förster
2. Prüfer: Dr. Yinguo Xiao

Table of Contents

List of figures

List of tables

List of abbreviations

MOF materials	$(CH_3)_2NH_2TM(HCOO)_3$ (with TM= Mn, Co, Mg, Ca)
AC	Alternating Current
Ca	Calcium
Co	Cobalt
Mg	Magnesium
Mn	Manganese
MOFs	Metal-Organic Frameworks
DMCaF	$(CH_3)_2NH_2Ca(HCOO)_3$
DMCoF	$(CH_3)_2NH_2Co(HCOO)_3$
$DMCo_{0.1}Mn_{0.9}F$	$(CH_3)_2NH_2Co_{0.1}Mn_{0.9}(HCOO)_3$
$DMCo_{0.2}Mn_{0.8}F$	$(CH_3)_2NH_2Co_{0.2}Mn_{0.8}(HCOO)_3$
DMMgF	$(CH_3)_2NH_2Mg(HCOO)_3$
DMMnF	$(CH_3)_2NH_2Mn(HCOO)_3$
DEPP	Dielectric Option Probe
SPPP	Spontaneous Polarization Option Probe

Abstract

The present thesis provides the investigations on the dielectric properties of multiferroic metal-organic framework (MOF) materials with formula MOFs $(CH_3)_2NH_2TM(HCOO)_3$ (with TM = Mn, Co, Mg, Ca). As a part of thesis work, the dielectric property measurement system is built up firstly based on a set of instruments including AH Capacitance Bridge, Keithley Electrometer, shielding box and sample holder. By combining with close cycle cooling system and LabVIEW controlling programs, the dielectric property measurement system can be used to carry out the measurements on the dielectric properties of ferroelectric samples in temperature range from 2 K to 300 K. The measurements on dielectric properties, including dielectric loss, capacitance, pyroelectric current and polarization, have been performed for different MOFs with different transition metal elements. It was found that the MOFs $(CH_3)_2NH_2TM(HCOO)_3$ (with TM = Mn, Co, Mg, Ca) exhibit different ferroelectric transition temperatures depending on the nature of transition metal elements. Compared with the transition temperature of MOF with lighter transition metal element, the MOF with larger atomic number of the transition metal element possesses lower transition temperature.

1 Introduction

Multiferroics, which possess both ferroelectric and ferromagnetic properties have gained growing attention since there may exist promising application potential in tunable multifunctional devices [1-3]. The most famous compounds displaying such behavior are oxide perovskites, such as $RMnO_3$ (R = Gd, Tb, Dy) [4]. Recently, Metal-Organic-Frameworks (MOFs) with perovskites architecture, i.e. $(CH_3)_2NH_2TM(HCOO)_3$ (with TM = Mn, Co, Mg, Ca), are identified as a new class of multiferroics [5].

The ferroelectric ordering in $(CH_3)_2NH_2TM(HCOO)_3$ occurs in the range of 160 K to185 K, whereas the long range magnetic ordering takes place in the temperature range from 8 K to 36 K attributed to the transition metal ions [5-6]. The ferroelectric phase transition appears to be driven by the ordering of hydrogen bonds linking the dimethyl ammonium cations. Multiferroic MOFs is considered as a promising multiferroics with potentially useful characteristics [7]. Moreover both the direct (magnetic field control of dielectric properties) and converse (electric field control of magnetization) magnetoelectric effects have been observed in the multiferroic state of multiferroic MOFs [8]. However, a clear picture of magnetic order state and the microscopic evidence for magnetoelectric coupling are still lacking due to the limitations of sample size and quality. In order to understand the dielectric properties of multiferroic MOFs with the perovskite architecture, it is significant to carry out dielectric property measurement on MOFs with different transition metal elements.

2 Theory

2.1 Metal-Organic Frameworks

MOFs is the abbreviation of Metal-Organic Frameworks. They are porous compounds that consist of organic clusters and inorganic metal ions, which are coordinated to organic ligands to form infinite systems. MOFs show different physical and chemical characteristic due to this porous structure. Particularly, the magnetic and electric properties of one type of the MOFs, which has the ABX_3 perovskite-like structure, can be adjusted in a simple crystalline structure, because the variable A and B components can provide the amount of space.

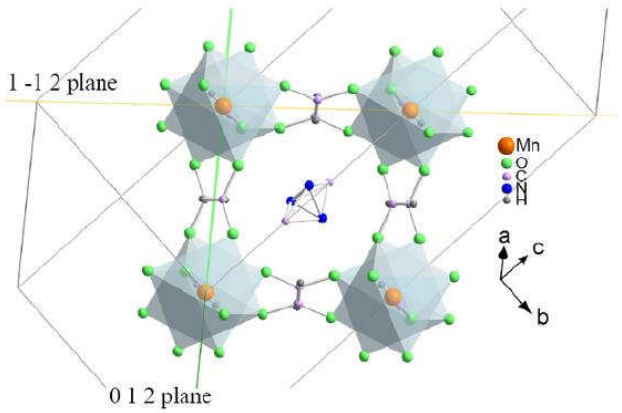

Figure 1: Illustration of crystal structure of MOFs $(CH_3)_2NH_2Mn(HCOO)_3$

Fig. 1 shows the crystal structure of MOFs $(CH_3)_2NH_2Mn(HCOO)_3$. In this structure, the ion Mn can be replaced by other metal ion. Plenty of room exists in the crystal structure. This is where the porous structure comes from. Because of the porous structure, these material are often used to store gas, separate poisonous gas, etc. In this work， there are six MOF samples with different transition metal elements need to be measured. They have a formula of $(CH_3)_2NH_2TM(HCOO)_3$ (with TM = Mn, Co, Mg or Ca). The geometric structure of single crystal sample is presented in Figure 2. The top view of sample is a parallelogram with two angles 95.8° and 84.2°. In this work, six samples have similar crystal structure.

Sample	Length/mm	Wide /mm	Area /mm^2	Thickness /mm
DMMnF	1.87	1.71	3.198	1.38
$DMCo_{0.1}Mn_{0.9}F$	1.77	1.58	2.797	0.88
$DMCo_{0.2}Mn_{0.8}F$	2.12	2.01	4.261	0.97
DMCoF	1.80	1.72	3.096	1.34
DMMgF	1.49	1.47	2.191	0.86
DMCaF	2.78	2.77	7.701	1.10

Table 1: Geometric data of samples

2.2 Dielectric properties

2.2.1 Capacitance

Capacitance is an electrical physical characteristic, which represents the ability of a material to store the electrical charge.

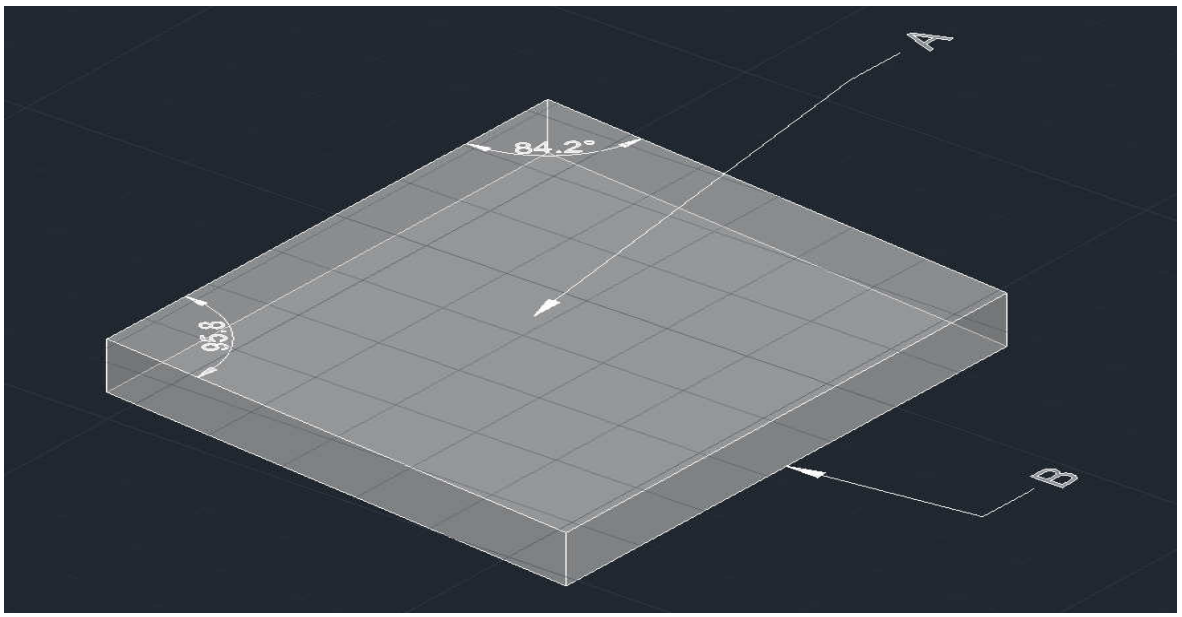

Figure 2: Geometric structure of sample

The capacitance between the top surface A and the bottom surface B need to be measurement.

2.2.2 Dielectric loss

Dielectric is an insulator in which electric dipoles are induced by an electric field. In general, dielectric loss is the loss of energy that propagates inside a dielectric material and convert into heat.

In general, the dielectric constant ε_r is a complex number given by

$$\varepsilon_r = \varepsilon_r' - j\varepsilon_r''$$

where, ε_r' is the real part and ε_r'' is the imaginary part. The dielectric loss is given by

$$\tan\delta = \frac{\varepsilon_r''}{\varepsilon_r'}$$

Real part ε_r' represents the relative permittivity (static dielectric contribution) in capacitance calculation; imaginary part ε_r'' represents the energy loss in a dielectric medium. Loss tangent tanδ represents how lossy the material is for AC signals [9].

2.2.3 Pyroelectric current and Polarization

In some material, the positive and negative charges in a crystal do not have their center at the same position in the unit cell. The rising or declining of temperature generates the pyroelectric current and changes the distance between the charges centers due to the thermal expansion or thermal contraction. A dielectric material can be electrically polarized upon the application of an electric field. This polarization occurs because electric dipoles orients themselves in response to the applied field. An internal electric field (blue *E*) is generated within the dielectric, which compensate the external electric field (red *E*).

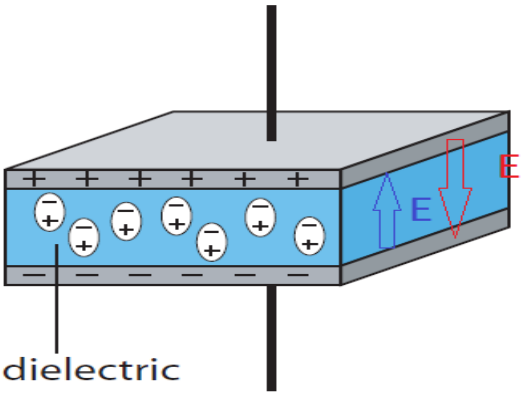

Figure 3: Illustration of electrical polarization

Measurements of the electric polarization are conducted by detecting the pyroelectric current I as a function of temperature. This current is proportional to the temperature change rate.

$$I = p(T)A\frac{\partial T}{\partial t}$$

Here, I is the current, A is the surface area of the electrodes on the sample, $\partial T/\partial t$ is the temperature change rate with respect to time, and $p(T)$ is defined as the pyroelectric coefficient at temperature T. The pyroelectric coefficient is also defined as the rate of change of the spontaneous polarization vector with respect to temperature [12]:

$$p(T) = \frac{\partial P_s}{\partial T}$$

The following relationship will be obtained after combining both equations, which are aforementioned.

$$P_s = \int \frac{Idt}{A}$$

After integrating the data from final time to start time, polarization can be obtained.

3 Experiment

3.1 Setup

3.1.1 AH Capacitance Bridge

The AH 2700A offers unparalleled stability, resolution, linearity and accuracy in a multi-frequency capacitance/loss bridge (whether manual or automatic). The precision of the AH 2700A is creating new applications in calibration, science and production in a wide range of fields [10]. It can provide the frequency from 50 Hz to 20 kHz. In this work, it is used to measure capacitance and dielectric loss in 1000 Hz.

Figure 4: AH 2700A Capacitance Bridge

3.1.2 Keithley Electrometer

The Keithley 6517A has extreme accuracy and sensitivity. It also offers a variety of features that simplify the measurement of high resistance and the resistivity of insulating materials [11]. The reading rates is up to 125 times per second. It provides a quick and easy way to measure low-level currents, such as pyroelectric current.

Figure 5: Keithley 6517A

When it provides voltage, the red lamp on the right side of the front part will be lighted.

3.1.3 Shielding box

Given the fact that the signal of pyroelectric current is very weak, it is necessary to find a proper method to reduce the noise from environment during the measurement. According to the instruction book of Keithley 6517A, the signal cable with the metal box is an optional method to shield the noise from outside.

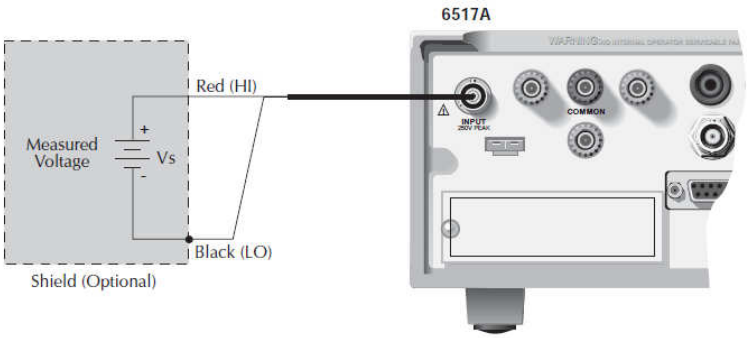

Figure 6: Shield method

The low noise cable is combined with a metal shielding box. The position 1, 2 and 3 are connected corresponding to high voltage, earth ground and low voltage. The shielding box is connected with the sample stick, which is introduced in 3.1.4.

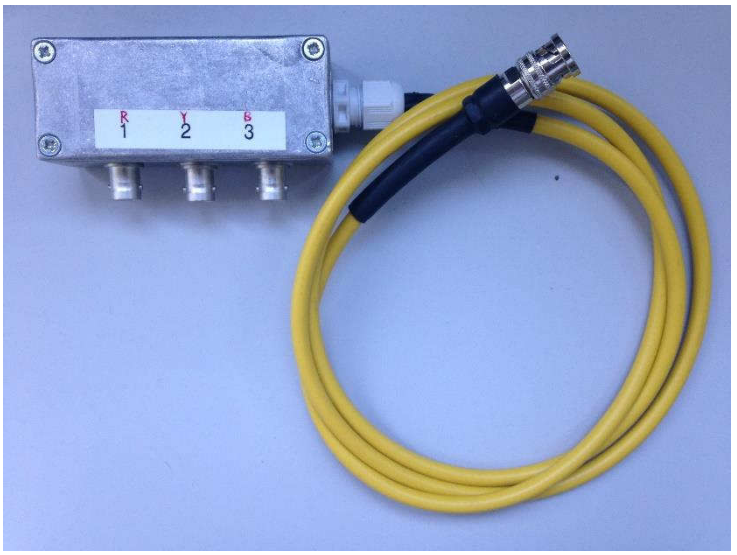

Figure 7: Shielding box and low noise cable

The background signal of pyroelectric current is roughly between $\pm 10^{-11}$ A. After using the shielding box, the background signal can be reduced to $\pm 10^{-13}$ A, which two orders of magnitude lower. The optimized background is sufficiently low and make the measurement of weak pyroelectric current signal feasible.

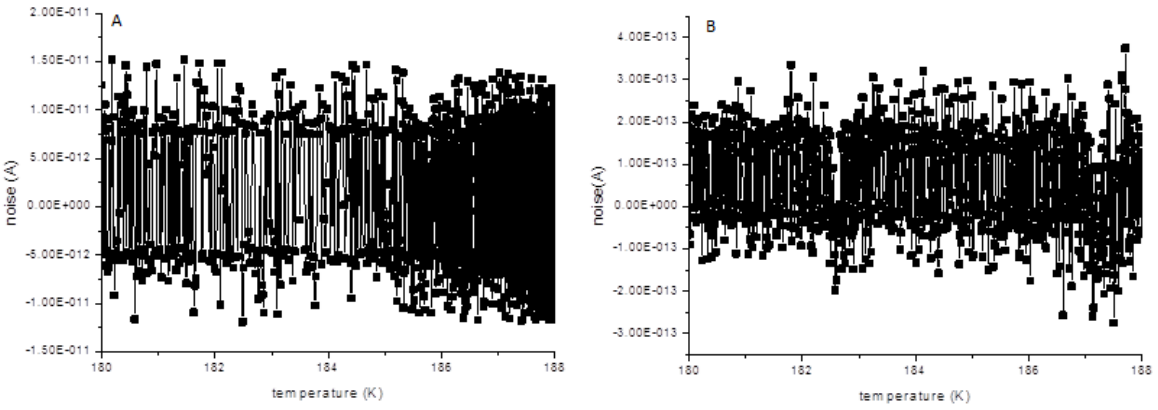

Figure 8: A: The noise of background without shielding box B: The noise of background with shielding box

3.1.4 Sample holder and Sample stick

The sample holder is in the small container at the bottom of sample stick. There is a copper plate in the middle of the sample holder, which is surrounded by four electrodes. The copper plate is connected with electrode 7 by silver paste, which is set as the negative electrode. In other words each holder can load three samples. The three samples are connected in corresponding to rest electrodes by platinum wire.

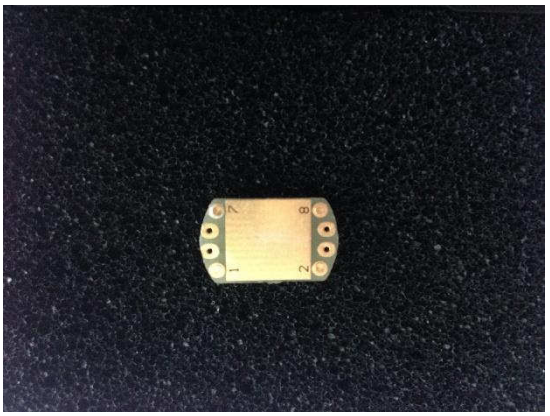

Figure 9: Sample holder

The sample stick is about 1.5 meters metal length. One side is the container, which is used to load the sample holder. Before the measurements, the container is evacuated to 0.1 mbar. The other side provides the cable interface. Number 0 is connecting port for thermal couple that used to read sample temperature. The connecting ports 1, 2, 3 and 4 are corresponding to electrodes on the sample holder 1, 2, 7 and 8.

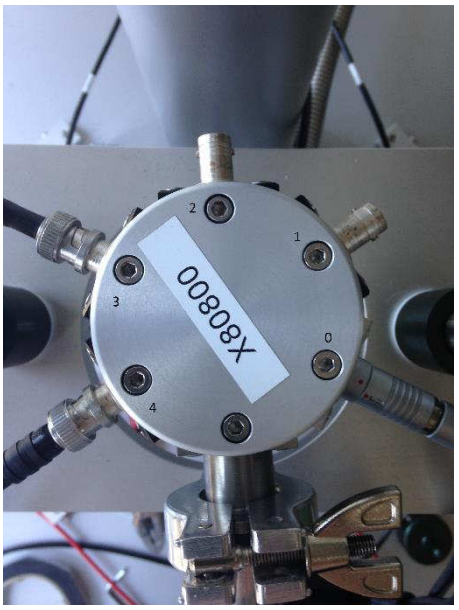

Figure 10: The top side of sample stick

3.2 Software

The measurements of capacitance, dielectric loss and pyroelectric current are controlled by the LabVIEW program.

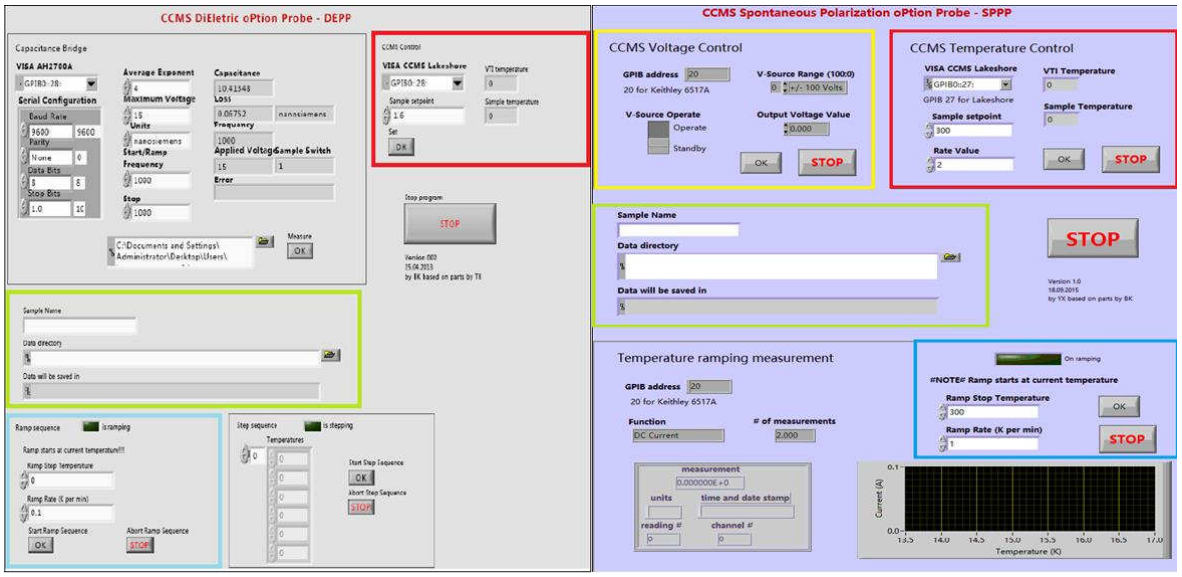

Figure 11: LabVIEW program of measurement

The DEPP (Dielectric Option Probe) is used to measure the dielectric loss and capacitance. The SPPP (Spontaneous Polarization Option Probe) is used to measure the pyroelectric current. Temperature of sample can be controlled by the interface in the red frame. The green frame is the storage path. The blue frame is used to set the ramp stop temperature and the ramp rate. The yellow frame is a place to provide the voltage for the step of cooling down, which is used to measure the pyroelectric current.

3.3 Measurement

The general condition of measurement is between 2 K and 300 K and the data is measured during warming up. The specific process is presented in 3.3.1 and 3.3.2.

Sample	Capacitance and Dielectric loss	Pyroelectric Current
DMMnF	From 2 K to 300 K, measurement during warming up	From 300 K to 2 K, cooling down in positive and negative voltage, then measurement from 2 K to 300 K without voltage
$DMCo_{0.1}Mn_{0.9}F$		
$DMCo_{0.2}Mn_{0.8}F$		
DMCoF		
DMMgF		
DMCaF		

Table 2: Measurement condition

3.3.1 Dielectric loss and Capacitance measurement

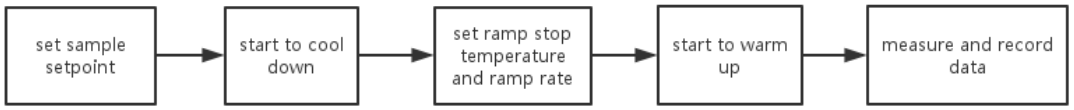

Figure 12: The process of dielectric loss and capacitance measurement

For the measurement of dielectric loss and capacitance setting the sample temperature is the first step. The objective temperature is 2 K. After reaching the target temperature set the ramp stop temperature as 300 K and ramp rate as 0.5 K per minute. The storage path also needs to write in the corresponding window. It will be measured by AH Capacitance Bridge, when the sample start to warm up. At the same time, the data is recorded by the computer. During the whole experiment, the frequency is set as 1000 Hz and the maximum voltage is 15 V.

3.3.2 Pyroelectric current measurement

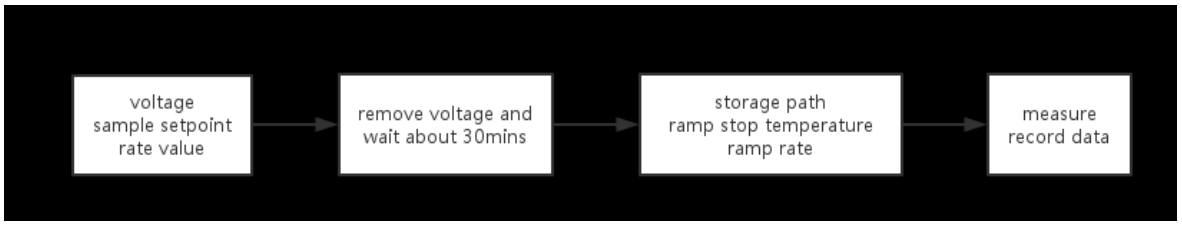

Figure 13: The process of pyroelectric current measurement

The objective temperature of the sample setpoint for the measurement of the pyroelectric current is 2 K. The ramping rate is set to be 10 K per minute. The poling electric field is loaded on the samples when the samples start to cool down. According to the thickness of the samples, the voltage on the samples is different.

Sample	**Electric Field / V**
DMMnF	±300
$DMCo_{0.1}Mn_{0.9}F$	±200
$DMCo_{0.2}Mn_{0.8}F$	±200
DMCoF	±100
DMMgF	±300
DMCaF	±300

Table 3: Electric field of each sample

After removing the poling electric field and releasing space charges for at least 30 minutes, the pyroelectric current was recorded during warming at a constant rate of 0.5 K per minute until 300 K.

4 Co-series samples

4.1 $(CH_3)_2NH_2Co_{0.1}Mn_{0.9}(HCOO)_3$

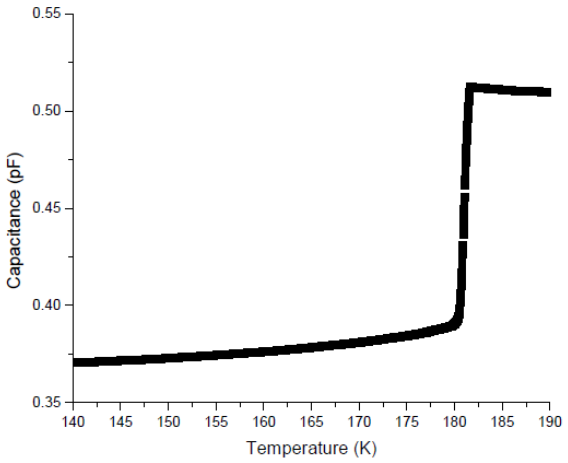

Figure 14: The change of capacitance in frequency 1000 Hz

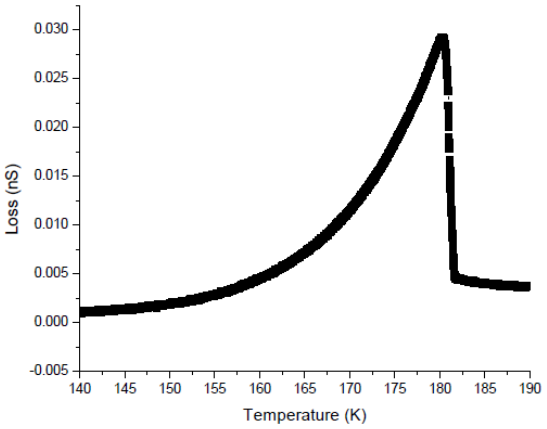

Figure 15: The change of dielectric loss in frequency 1000 Hz

In Fig. 14, the temperature dependence of capacitance has a sharp increase from approximately 0.385 pF to 0.515 pF between 180 K and 182 K. The rising capacitance is 0.13 pF. In Fig. 15, the temperature dependence of dielectric loss has an increase of similar quadratic function and a sharp decrease. The peak of dielectric loss is similar to 0.030 nS at the critical point of temperature about 180K.

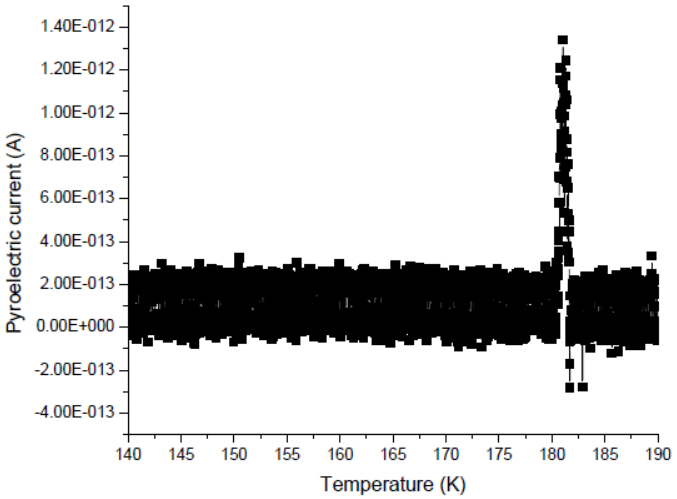

Figure 16: Pyroelectric current after poling with positive electric field 200 V

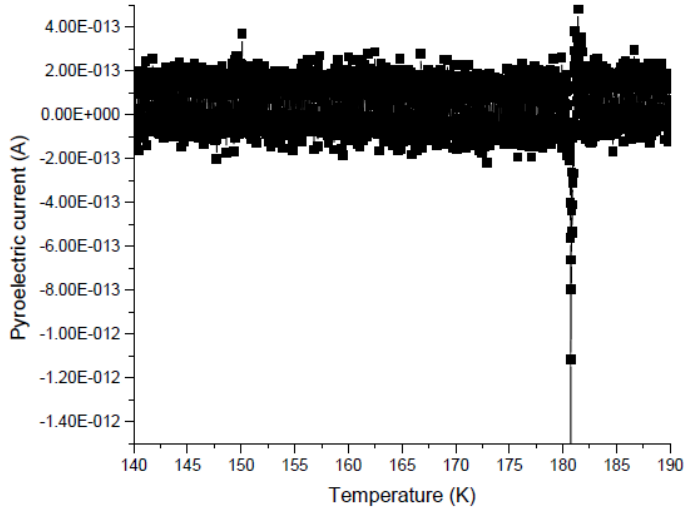

Figure 17: Pyroelectric current after poling with negative electric field -200 V

The sharp peak of pyroelectric current in the positive poling electric field 200 V is approximately 1.4×10^{-12} A at about 180 K. The sharp anomaly peak of pyroelectric current in the negative poling electric field -200 V is approximately -1.5×10^{-12} A at about 180 K. Fig. 16 and Fig. 17 are generally symmetric.

The value of the pyroelectric current depends on the value of poling electrical field. A higher voltage leads to a stronger signal of the pyroelectric current. By using positive poling electrical field can obtain a positive signal of the pyroelectric current. A negative poling electric field leads to a negative signal of the pyroelectric current. Above the ferroelectric transition temperature, the signal becomes flat, which indicates that the paraelectric state is established and electrical polarization no longer exists in the sample.

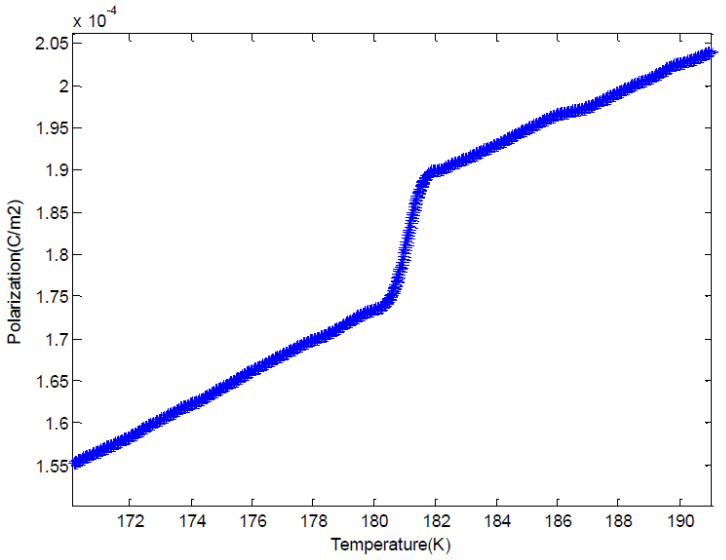

Figure 18: Polarization of pyroelectric current with positive poling electric field

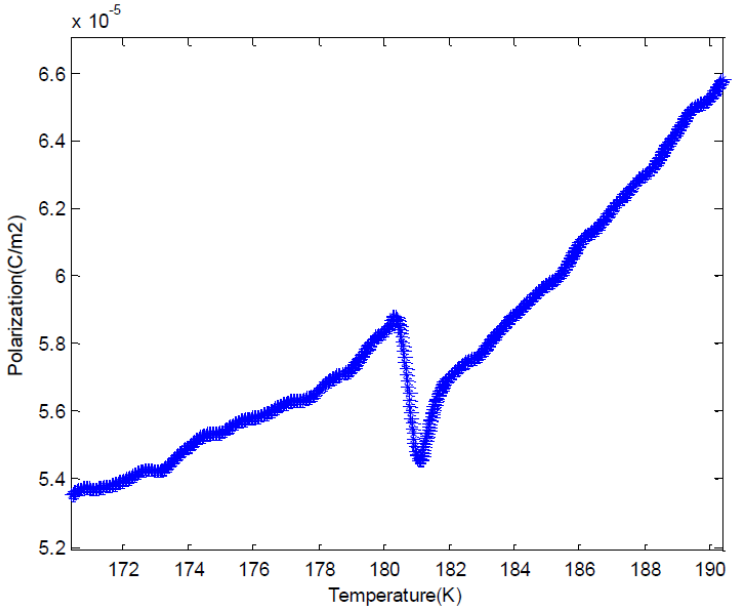

Figure 19: Polarization of pyroelectric current with negative poling electric field

Basically, the polarization is linearly increasing. However, there is a sharp anomaly change between temperature 180 K and 182 K. The polarization rises from 1.75×10^{-4} C/m^2 to 1.90×10^{-4} C/m^2 because of the positive poling electric field. The polarization decreases roughly from 5.9×10^{-5} C/m^2 to 5.4×10^{-5} C/m^2 because of the negative poling electric field.

4.2 $(CH_3)_2NH_2Co_{0.2}Mn_{0.8}(HCOO)_3$

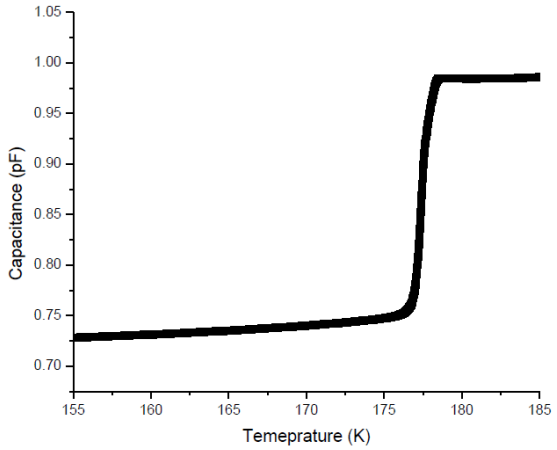

Figure 20: The change of capacitance in frequency 1000 Hz

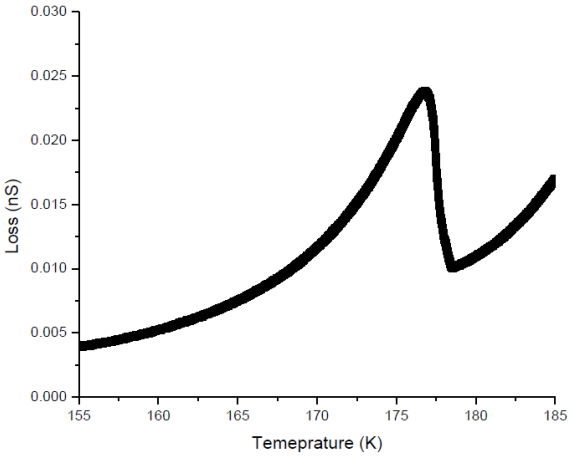

Figure 21: The change of dielectric loss in frequency 1000 Hz

In Fig. 20, the temperature dependence of capacitance has a sharp increase from approximately 0.75 pF to 0.98 pF between 177 K and 178 K. The rising capacitance is 0.23 pF. In Fig. 21, the temperature dependence of dielectric loss has an increase of similar quadratic function and a sharp decrease. The peak of dielectric loss is similar to 0.025 nS at the critical point of temperature about 177 K.

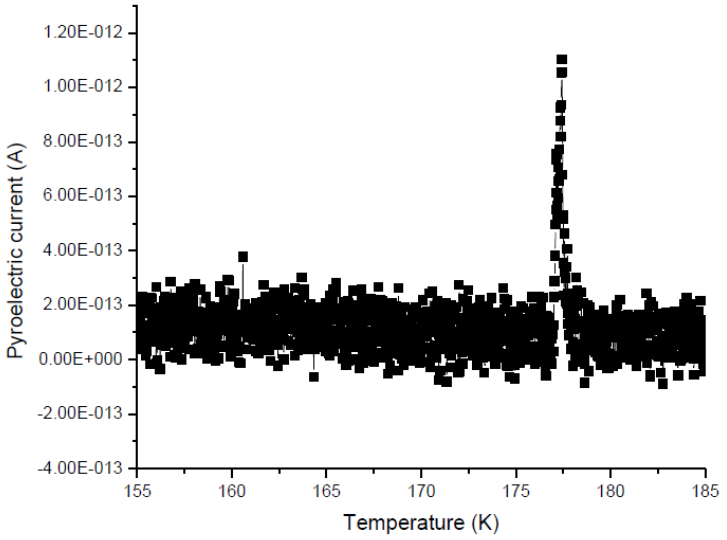

Figure 22: Pyroelectric current after poling with positive electric field 200 V

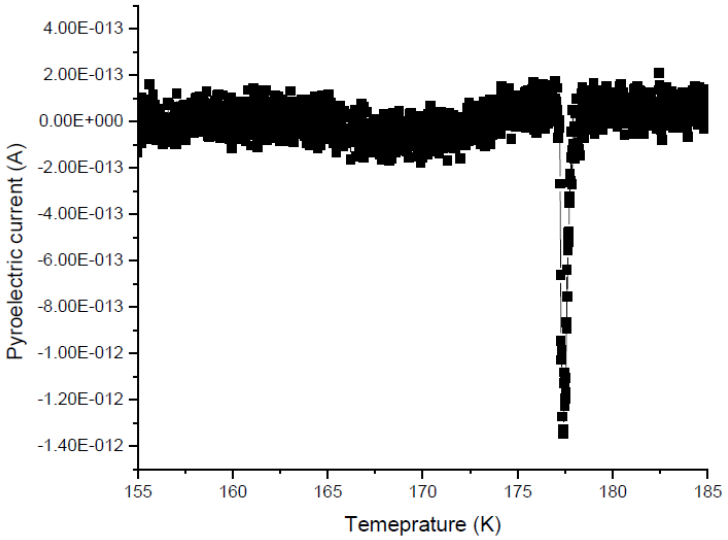

Figure 23: Pyroelectric current after poling with negative electric field -200 V

The sharp anomaly peak of pyroelectric current in the positive poling electric field 200 V is approximately 1.1×10^{-12} A at about 177 K. The sharp anomaly peak of pyroelectric current in the negative poling electric field -200 V is approximately -1.4×10^{-12} A at about 177 K. Fig. 22 and Fig. 23 are generally symmetric.

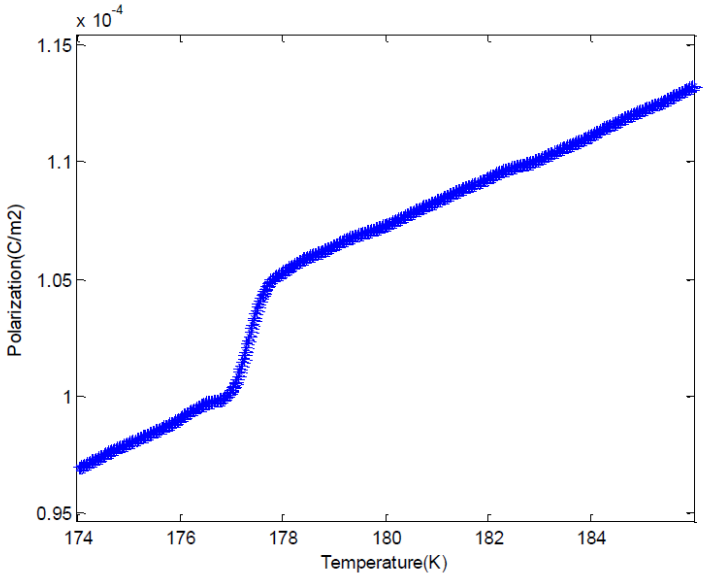

Figure 24: Polarization of pyroelectric current with positive poling electric field

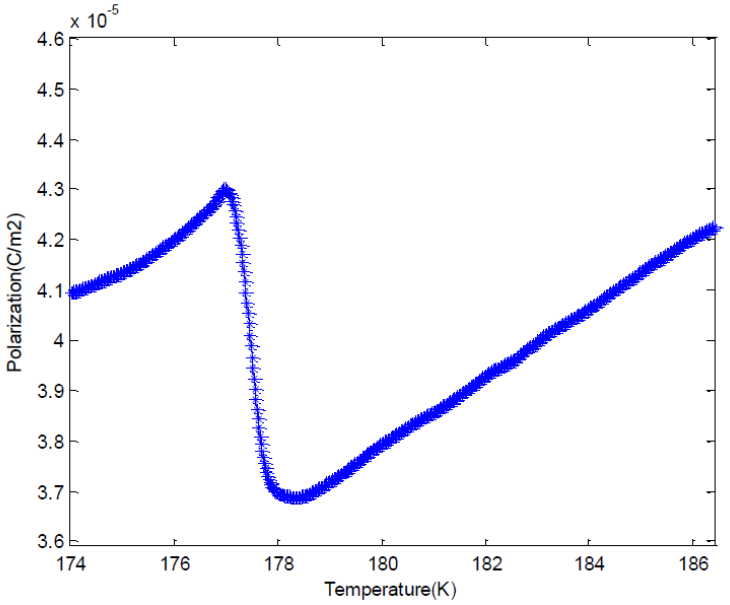

Figure 25: Polarization of pyroelectric current with negative poling electric field

Basically, the polarization is linearly increasing. However, there is a sharp anomaly change between temperature 177 K and 178 K. The polarization rises from 1.00×10^{-4} C/m^2 to 1.05×10^{-4} C/m^2 because of the positive poling electric field. The polarization decreases roughly from 4.3×10^{-5} C/m^2 to 3.7×10^{-5} C/m^2 because of the negative poling electric field.

4.3 $(CH_3)_2NH_2Co(HCOO)_3$

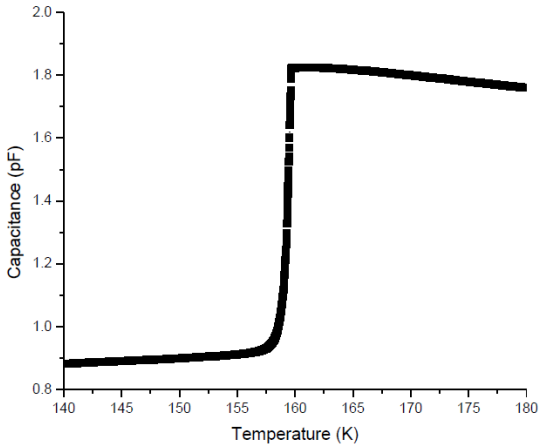

Figure 26: The change of capacitance in frequency 1000 Hz

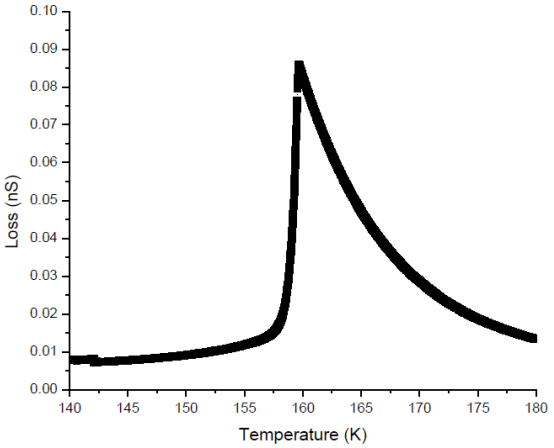

Figure 27: The change of dielectric loss in frequency 1000 Hz

In Fig. 26, the temperature dependence of capacitance has a sharp increase from approximately 0.95 pF to 1.80 pF between 158 K and 160 K. The rising capacitance is 0.85 pF. In Fig. 27, the temperature dependence of dielectric loss has an increase of similar quadratic function and a sharp decrease. The peak of dielectric loss is similar to 0.087 nS at the critical point of temperature about 160 K.

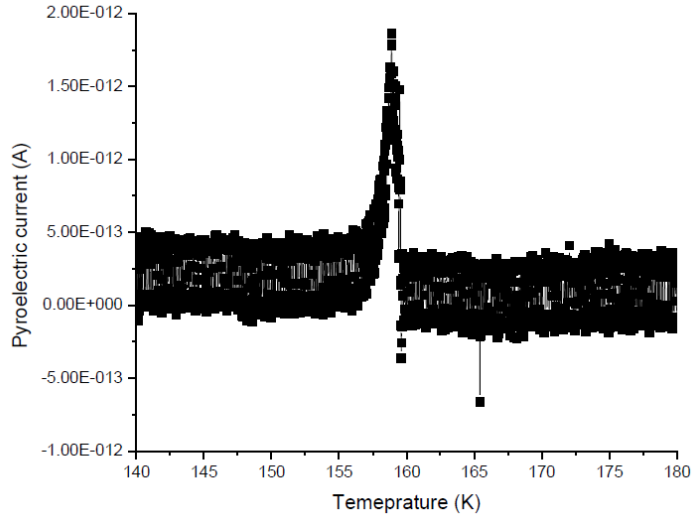

Figure 28: Pyroelectric current after poling with positive electric field 100 V

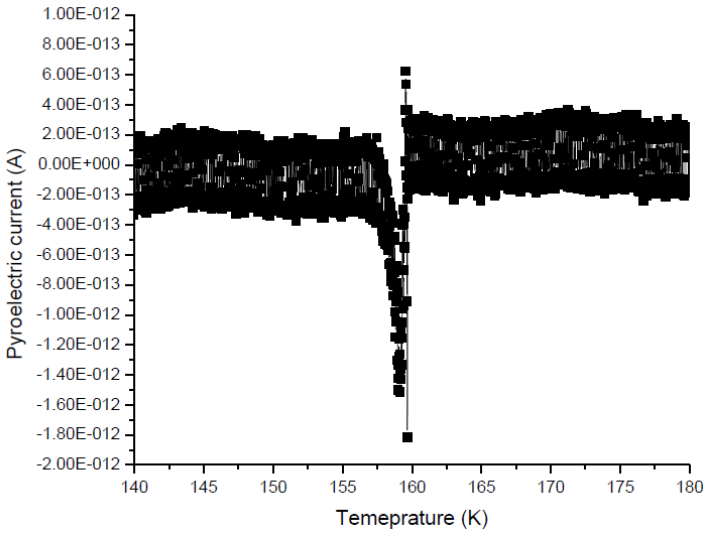

Figure 29: Pyroelectric current after poling with negative electric field -100 V

The sharp anomaly peak of pyroelectric current in the positive poling electric field 100 V is approximately 1.8×10^{-12} A at about 160 K. The sharp anomaly peak of pyroelectric current in the negative poling electric field -100 V is approximately -1.8×10^{-12} A at about 160 K. Fig. 28 and Fig. 29 are generally symmetric.

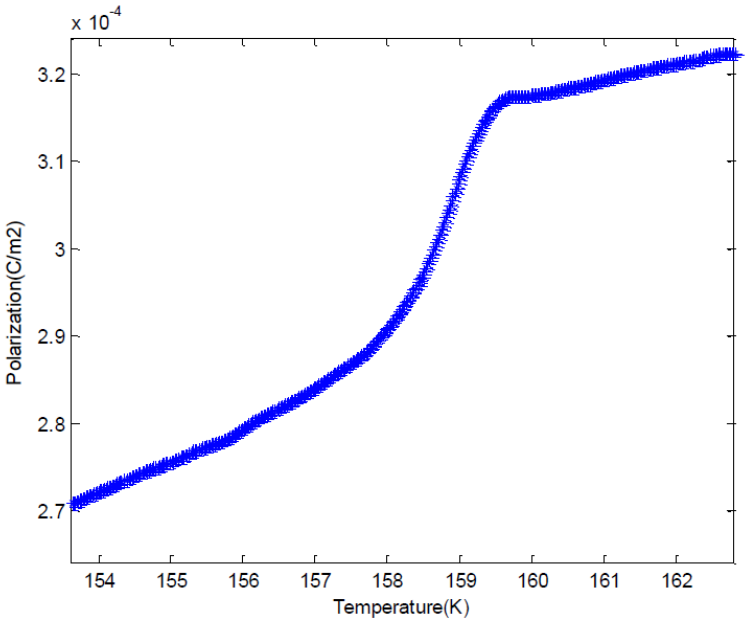

Figure 30: Polarization of pyroelectric current with positive poling electric field

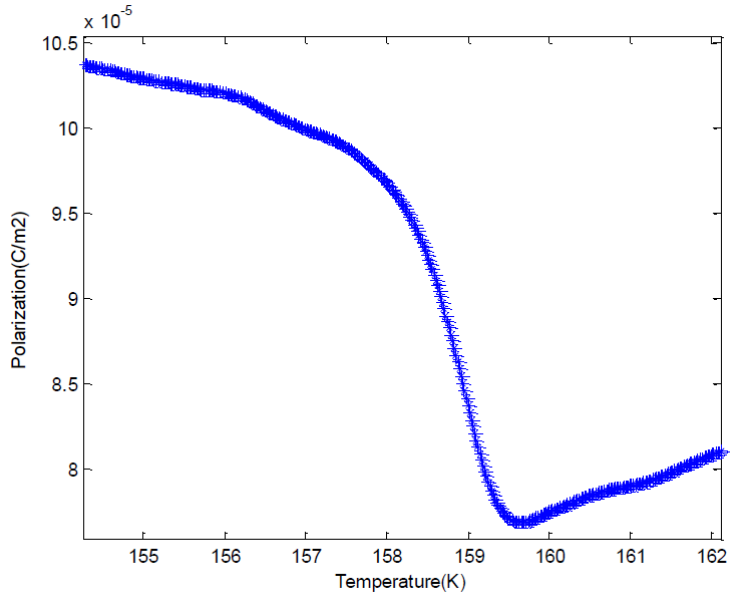

Figure 31: Polarization of pyroelectric current with negative poling electric field

In Fig. 30, an increase of similar quadratic function ends about 159.5 K, then it shows a linearly increase trend. In Fig. 31, a decrease of similar quadratic function also ends about 159.5 K, then it shows a linearly increase trend.

5 Single metallic element samples

5.1 $(CH_3)_2NH_2Mg(HCOO)_3$

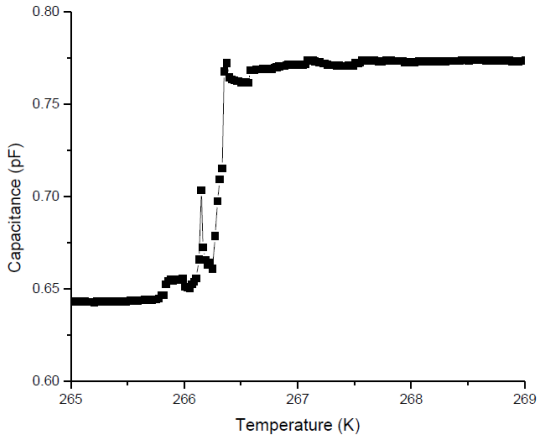

Figure 32: The change of capacitance in frequency 1000 Hz

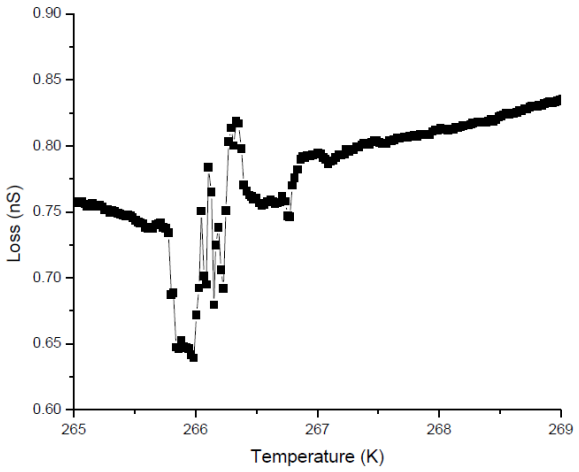

Figure 33: The change of dielectric loss in frequency 1000 Hz

The temperature dependence of capacitance starts to sharply rise at about 266 K and ends at about 266.5 K. In correspondence with capacitance increases from 0.65 pF to 0.77 pF. In general, although the rising path of dielectric loss is not clear, it can be found that it starts from 0.64 nS at 266 K and arrives the peak 0.82 nS at 266.3 K, which is also the beginning of decrease.

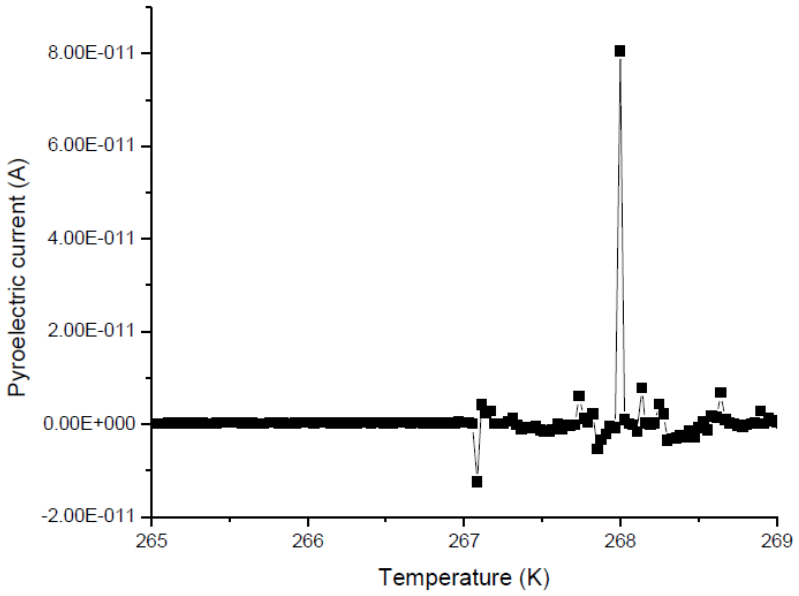

Figure 34: Pyroelectric current after poling with positive electric field 300 V

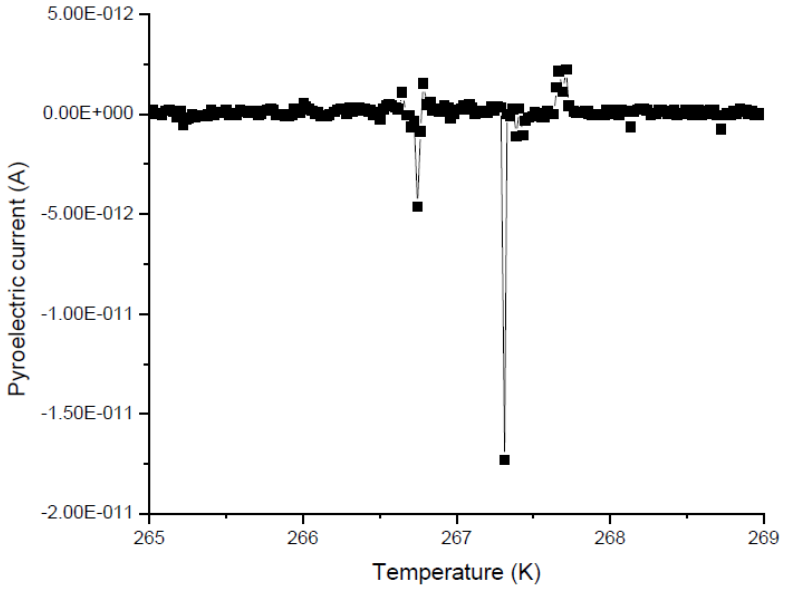

Figure 35: Pyroelectric current after poling with negative electric field -300 V

The peak pyroelectric current with positive poling electric field 300 V at approximately 268 K is 8×10^{-11} A. The peak pyroelectric current with negative poling electric field -300 V at approximately 267.3 K is -1.75×10-11 A. Two values of temperature have a little difference.

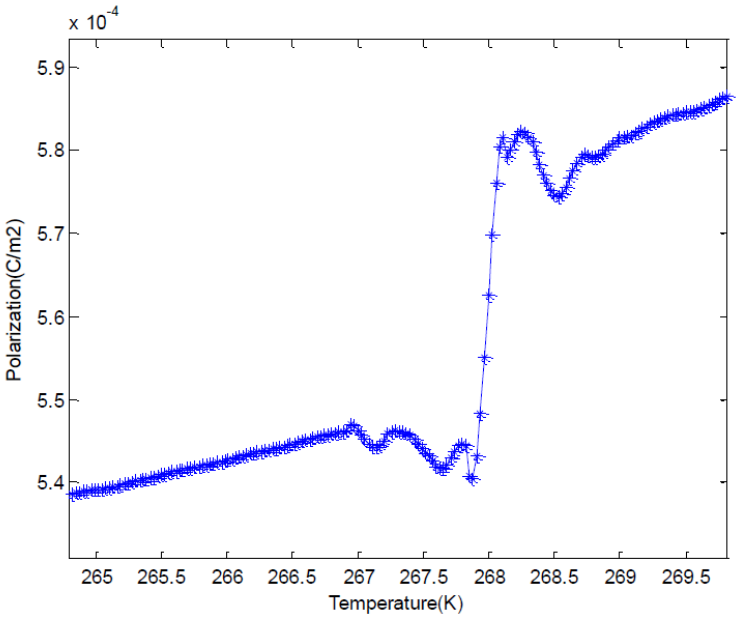

Figure 36: Polarization of pyroelectric current with positive poling electric field

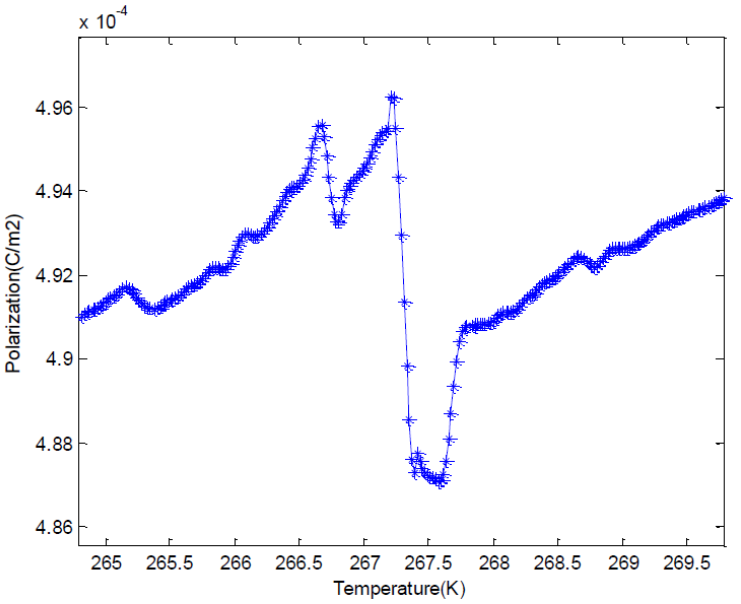

Figure 37: Polarization of pyroelectric current with negative poling electric field

Basically, the polarization is linearly increasing. However, there is a sharp anomaly change between temperature 267.9 K and 268.1 K in Fig. 36. The polarization rises from 5.4×10^{-4} C/m^2 to 5.8×10^{-4} C/m^2. A sharp anomaly change exists between 267.2 K and 267.5 K in Fig. 37. The polarization decreases roughly from 4.96×10^{-4} C/m^2 to 4.87×10^{-4} C/m^2 because of the negative poling electric field.

5.2 $(CH_3)_2NH_2Ca(HCOO)_3$

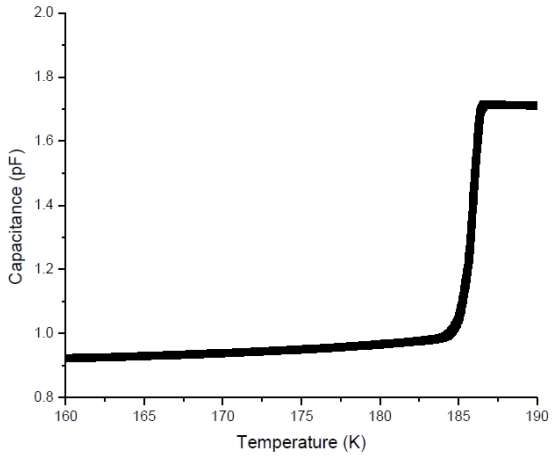

Figure 38: The change of capacitance in frequency 1000 Hz

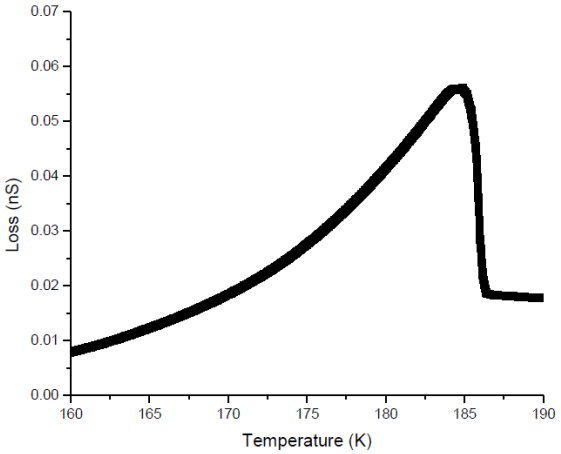

Figure 39: The change of dielectric loss in frequency 1000 Hz

In Fig. 38, the temperature dependence of capacitance has a sharp increase from approximately 1.0 pF to 1.7 pF between 185 K and 187 K. The rising capacitance is 0.7 pF. In Fig. 39, the temperature dependence of dielectric loss has an increase of similar quadratic function and a sharp decrease. The peak of dielectric loss is similar to 0.055 nS at the critical point of temperature about 185 K.

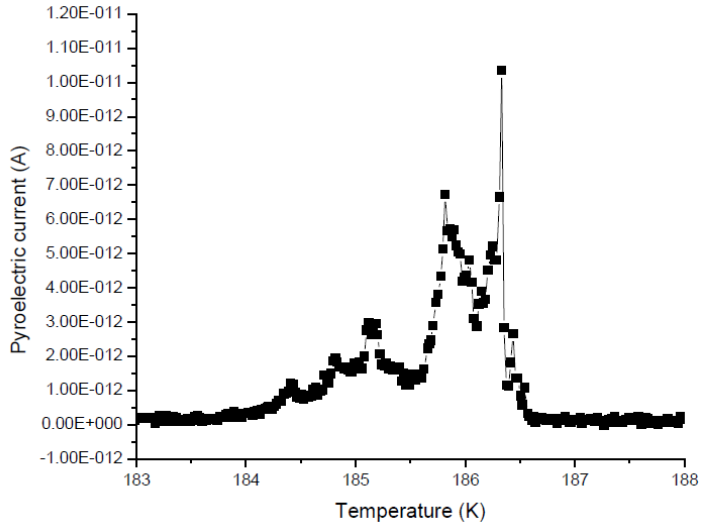

Figure 40: Pyroelectric current after poling with positive electric field 300 V

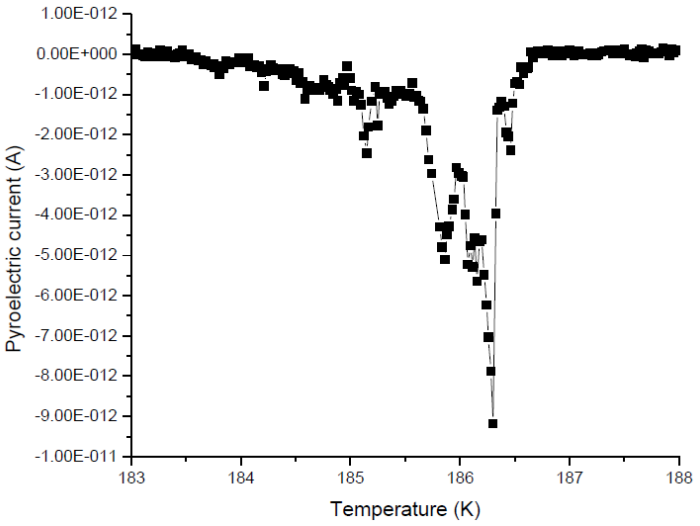

Figure 41: Pyroelectric current after poling with negative electric field -300 V

The sharp anomaly peak of pyroelectric current in the positive poling electric field 300 V is approximately 1.05×10^{-11} A at about 186.3 K. The sharp anomaly peak of pyroelectric current in the negative poling electric field -300 V is approximately -0.95×10^{-11} A at about 186.3 K. Fig. 40 and Fig. 41 are generally symmetric.

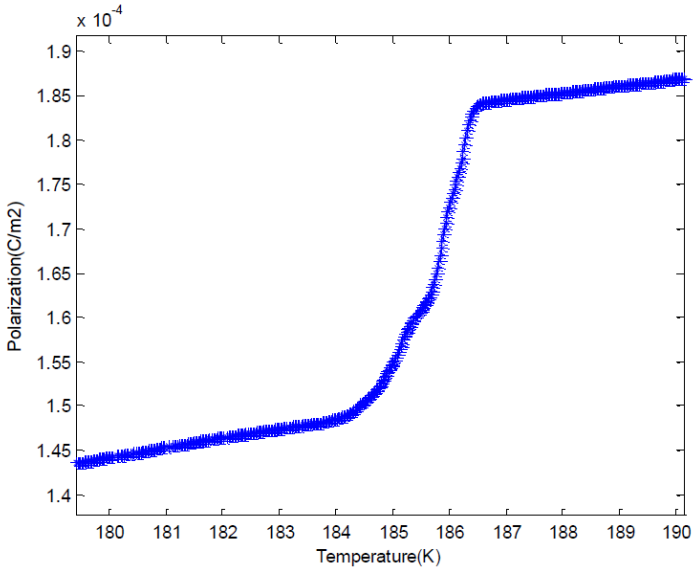

Figure 42: Polarization of pyroelectric current with positive electric field

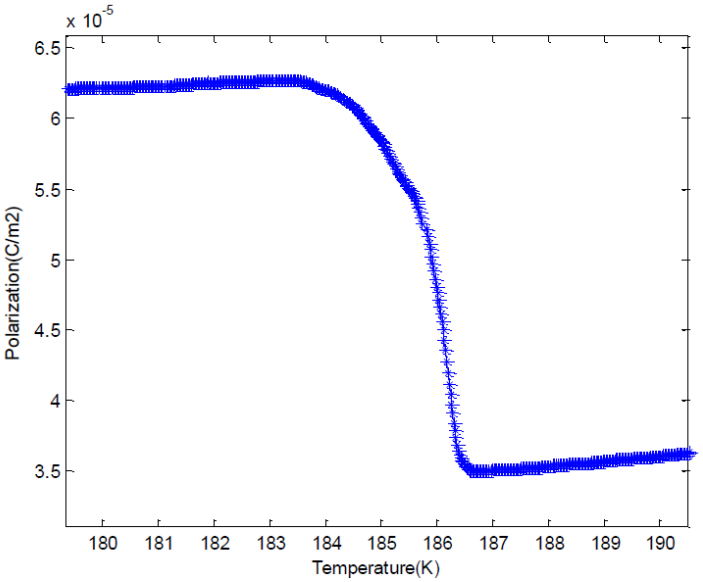

Figure 43: Polarization of pyroelectric current with negative electric field

Both polarizations can be considered as stable lines except at the period where the temperature is between 184.0 K and 186.5 K. In this period, the polarization rises from 1.47×10^{-4} C/m^2 to 1.85×10^{-4} C/m^2 with pyroelectric current in the positive poling electric field and decreases from 6.2×10^{-5} C/m^2 to 3.5×10^{-5} C/m^2 with pyroelectric current in the negative poling electric field.

5.3 $(CH_3)_2NH_2Mn(HCOO)_3$

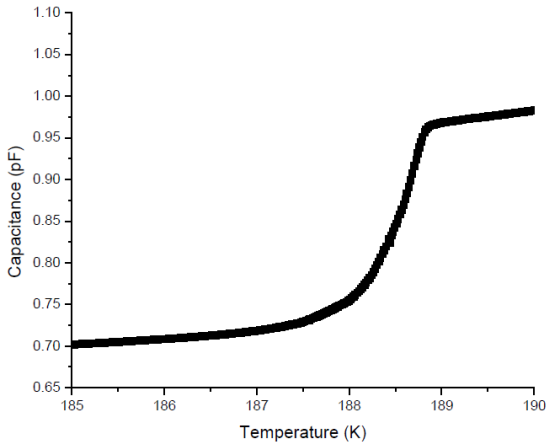

Figure 44: The change of capacitance in frequency 1000 Hz

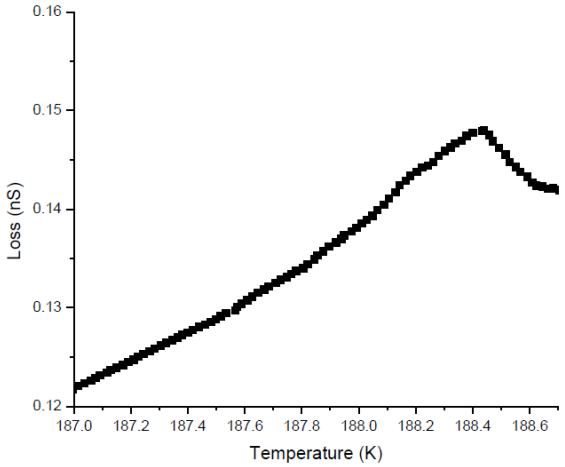

Figure 45: The change of dielectric loss in frequency 1000 Hz

In Fig. 44, the temperature dependence of capacitance has a sharply increase from approximately 0.75 pF to 0.96 pF between 187 K and 189 K. The rising capacitance is 0.21 pF. In Fig. 45, the temperature dependence of dielectric loss has an increase that ends to 0.148 nS at 188.4 K.

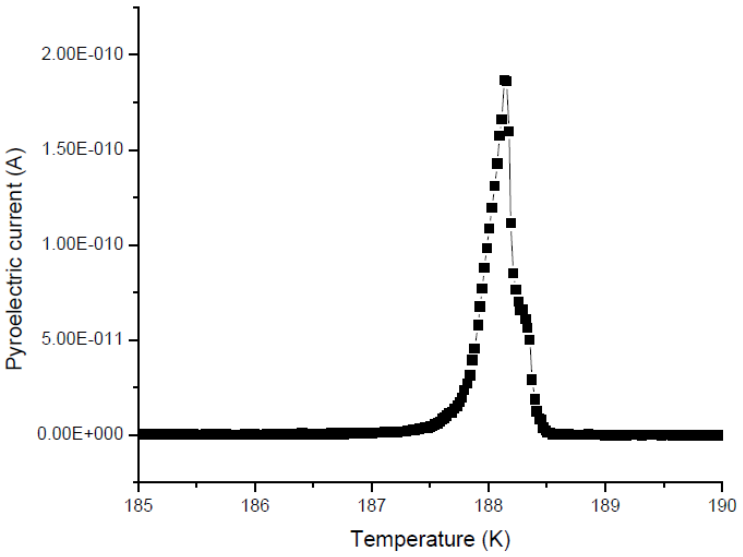

Figure 46: Pyroelectric current after poling with positive electric field 300 V

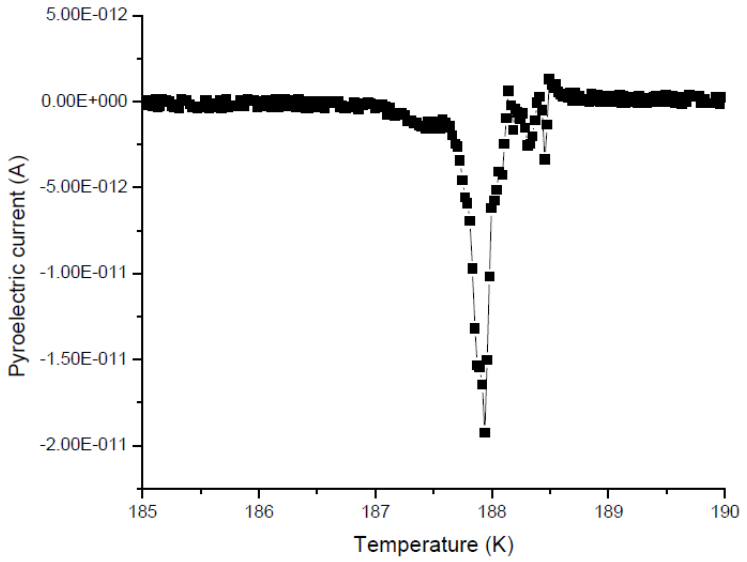

Figure 47: Pyroelectric current after poling with negative electric field -300 V

The sharp anomaly peak of pyroelectric current in the positive poling electric field 300 V is approximately 1.85×10^{-10} A at about 188.1 K. The sharp anomaly peak of pyroelectric current in the negative poling electric field -300 V is approximately -1.95×10^{-11} A at about 187.9 K.

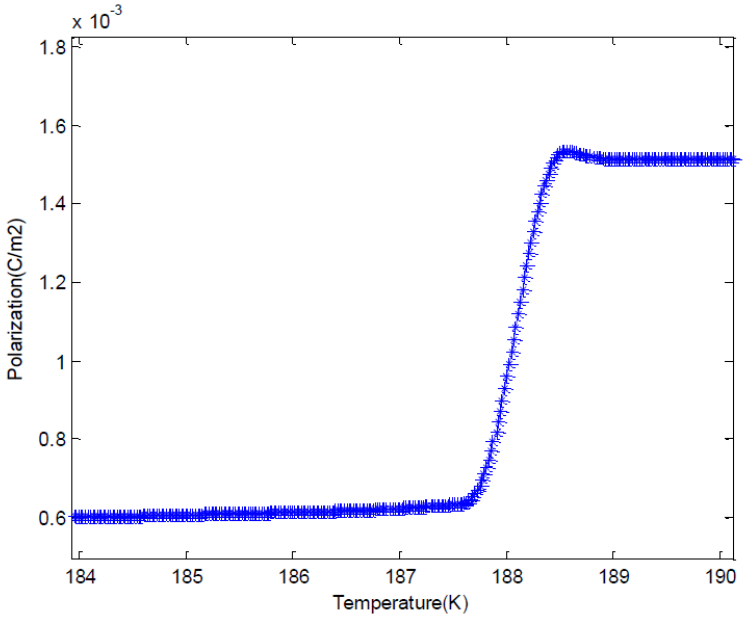

Figure 48: Polarization of pyroelectric current with positive poling electric field

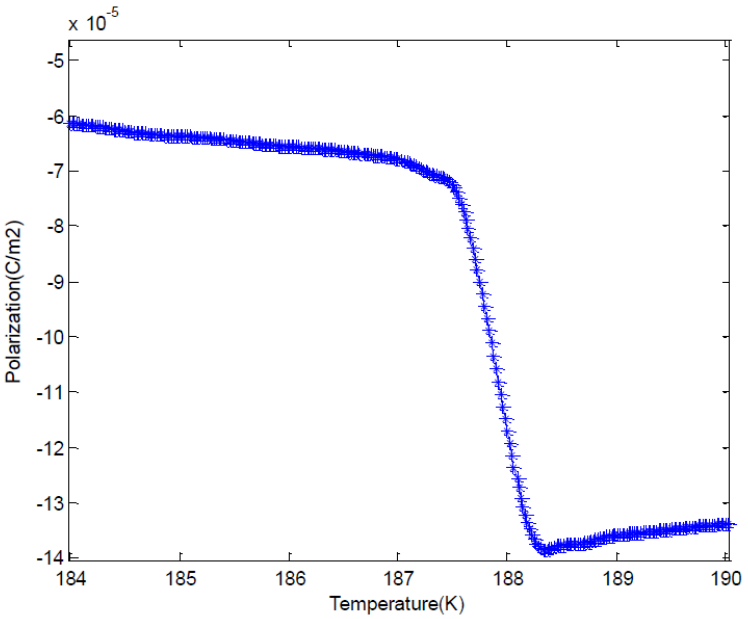

Figure 49: Polarization of pyroelectric current with negative poling electric field

Both polarizations can be considered as stable lines except at the period where the temperature is between 187.5 K and 188.5 K. In this period, the polarization rises from 0.6×10^{-3} C/m^2 to 1.5×10^{-3} C/m^2 with pyroelectric current in the positive poling electric field and decreases from -0.7×10^{-4} C/m^2 to -1.4×10^{-4} C/m^2 with pyroelectric current in the negative poling electric field.

6 Conclusions

From the dielectric property measurements of Co-based MOF samples, it was shown that all of the investigated samples exhibit anomalies in capacitance, dielectric loss and pyroelectric current, indicating the existence of ferroelectric phase transition. It is also found that the transition temperature is different for samples with different compositions. The transition temperature becomes lower as the concentration of cobalt increases. The concentration of cobalt in MOF samples influence not only the ferroelectric transition temperature but also the magnitudes of dielectric loss and capacitance. In general, the increasing cobalt content leads to higher values of dielectric loss and capacitance of MOF samples.

For MOF samples with different transition metal elements, such as magnesium, calcium and manganese, the sharp anomalies in dielectric loss and capacitance are also observed. For each specific sample, the anomalies in dielectric loss and capacitance take place in the same temperature, indicating the ferroelectric to paraelectric phase transition in these compounds. The transition temperature are different for MOFs with different transition metal elements. By comparison of dielectric properties of all MOFs, it can be found that the bigger the atomic number of the transition metal element in the sample the lower is the ferroelectric transition temperature.

Bibliography

[1] T. Kimura *et al*., Nature(London) 426, 55(2003).

[2] M. Fiebig, J. Phys. D 38, R123(2005).

[3] Y. Tokura and S. Seki, Adv. Mater. 22, 1554(2010).

[4] T. Goto *et al*., Phys. Rev. Lett. 92, 257201(2004).

[5] P. Jain *et al*., J. Am. Chem. Soc. 131, 13625(2009).

[6] X.-Y. Wang *et al*., Inorg. Chem. 43, 4615(2004).

[7] R. Ramesh, Nature 461, 1218(2009).

[8] Y. Tian *et al*., Sci. Rep. 4, 6062(2014).

[9] Zhu Chunxiang: Dielectric loss. [Online]. Available: http://faculty.kfupm.edu.sa/EE/zhamouz/051/EE620-051/others/2_Dielectric_loss.pdf (07.08.2016).

[10] AH 2700A, http://www.andeen-hagerling.com/ah2700a.htm , 18.08.2016.

[11] Keithley 6517A, http://www.axiomtest.com/Meters/Digital-Multimeter-(DMM)-and-Digital-Voltmeter/Keithley/6517A/Electrometer-..-High-Resistance-Meter/ , 20.08.2016.

[12] Daniel Thomas O'Flynn: Multiferroic properties of rare earth manganites. September 2010.